JOHNSON MATTHEY
TECHNOLOGY REVIEW

www.technology.matthey.com

Johnson Matthey's international journal of research exploring science and technology in industrial applications

**********Accepted Manuscript**********

This article is an accepted manuscript

It has been peer reviewed and accepted for publication but has not yet been copyedited, house styled, proofread or typeset. The final published version may contain differences as a result of the above procedures

It will be published in the **JANUARY 2022** issue of the *Johnson Matthey Technology Review*

Please visit the website https://www.technology.matthey.com/ for Open Access to the article and the full issue once published

Johnson Matthey Technology Review
Johnson Matthey Plc
Orchard Road
Royston
SG8 5HE
UK
Tel +44 (0)1763 253 000
Email tech.review@matthey.com

<https://doi.org/10.1595/205651322X16212512135401 >

<First page number: TBC>

Adsorption of Transition Metal Catalysts on Carbon Supports: A Theoretical Perspective

Arunabhiram Chutia*

School of Chemistry, University of Lincoln, Brayford Pool, Lincoln, LN6 7TS, UK

*Email: achutia@lincoln.ac.uk

ABSTRACT

Adsorption is a fundamental process, which takes place on a catalyst surface before it dissociates, diffuses over the surface and recombines with other adsorbed species to form the final product. Therefore, in theoretical chemistry understanding of the local geometrical and electronic properties of the adsorbed species on the catalyst surface has been a topic of core focus. In this short review we briefly summarise some of the important developments on theoretical studies related to the adsorption properties of transition metal catalysts on graphene and graphene-related carbon materials. Prior to this, we will present a discussion on various forms of carbon materials used as catalyst supports, which will be followed by a brief discussion of the fundamentals of the density functional theory.

1. Introduction

As early as 1834 Michael Faraday performed some of the original studies on adsorption, which is a fundamental surface phenomenon involving the interaction of atoms and molecules from vapour phases or a solution, onto the surfaces and pores of solids (1). It is now well-known that adsorption can be either physisorption (also referred as van der Waals adsorption or physical adsorption) or chemisorption. In physisorption, as the name suggests, the weak physical van der Waals forces are involved, and the heat evolved during this process is usually very small. Chemisorption on the other hand, first studied by Irving Langmuir in 1916, occurs due to the formation of chemical bonds between the adsorbate and adsorbent and the heat evolved during this process is significantly higher (in the range of 100 – 500 kJ/mol). So far numerous theoretical studies have been performed to understand the adsorption properties of atoms, clusters and molecules on catalyst surfaces (2) (3–14). However, in this short review we will focus only on the density functional theory (DFT) based studies on the adsorption properties of transition metal catalysts on graphene and discuss the future of similar studies on amorphous carbon materials where graphene is the basic structural unit. First, we will present a brief summary of the physical and chemical features of various carbon materials widely used as catalyst supports, which will be followed by a brief discussion on DFT.

1.1. Graphite and graphene

The word graphene refers to a single atomic plane of graphite and the word graphite has its origin in the Greek word "Γραφειη" (pronounced as graphein), which means to draw or to write.(15) Graphite is one of the first known materials to be studied using

X-ray diffraction by A. W. Hull in 1917(16). He proposed that the normal structure of graphite has hexagonal D_{6h} symmetry (16). Later this structure was confirmed by J. D. Bernal and O. Hessel and Z. H. Mark in 1924(17),(18). According to their model of graphite, it consists of a stack of parallel hexagonal net planes of carbon atoms with C-C bond length of 1.42 Å and these net planes are separated by a distance of 3.35 Å and the unit cell contains four atoms in a planar stacking sequence ABABA… However, later reports based on X-ray spectroscopy accounted for these hexagonal planes being stacked in ABCABC … sequence (19)(20)(21)(22)(23)(24). These reports revealed that in ordinary temperatures and pressures natural graphite occurs in two crystal structures (a) Bernal with an ABABA … sequence of arrangements and (b) rhombohedral with an ABCABC… sequence of arrangements(25).

During the early period of research on graphite, many studies on its physical properties were also reported. For example, in 1915 G. E. Washburn measured the electrical resistance parallel to the basal plane of a perfect sample approximating to single crystals or highly oriented polycrystalline samples (26). Similar reports on electrical resistance measurements were reported by Ryschkewitsch in 1923 (27). Measurements related to the temperature-dependence of the electrical resistance parallel to the layers, were made by D. E. Roberts in 1913 and W. Meissner, H. Franz and H. Westerhof in 1932. In these reports the resistivity was found in the range of 4-8 × 10^{-5} ohm-cm. Later, G. E. Washburn and N. Ganguli and K. S. Krishnan reported that the resistivity perpendicular to the basal plane was 10^2 - 10^3 times greater than that of the parallel planes (28). Simultaneous theoretical studies to explore the

electronic structure of graphite were also carried out. The first known energy band structure of graphite crystal was studied as early as 1935 by Hund and Mrowka (29). However, the first known theoretical calculations with an attempt to relate them to properties such as electrical conductivity of graphite were made by Wallace and Coulson in 1947 (30)(31). Wallace employed "tight-binding" approximation to develop the electronic energy bands and Brillouin zones of graphite (32).

In addition to the investigations on the structural, physical and electronic properties, the history of studies on the chemical properties of graphite such as the reaction of graphite with gases, particularly oxygen and carbon dioxide in presence of catalysts was also reported, but the use of graphite as catalyst support was seen much later (33). For example, Brownlie *et al*. used graphite as a catalyst support to investigate how properties of metals are influenced by its interaction with the surface (32). Under standard temperatures and pressures, graphite is the most stable allotrope of carbon but due to its low surface area it was used very little as catalyst support (34).

In recent years however, many studies on the use of expanded graphite as catalyst supports have been reported (34),(35). We note that a modified graphite having an enlarged interlayer lattice distance of 4.3Å, and has a long-range-order layered structure of graphite is referred to as expanded graphite (36). For example, Chen *et al* recently showed that PtCo nanoparticles supported on expanded graphite have higher electrocatalytic activity and antipoisoning ability and long-term stability for methanol oxidation (35). The expanded graphite also finds its application in fuel cell electrode material due to its good electrical and thermal conductivity, chemical stability

and excellent mechanical properties (37). Other interesting experimental studies have been also reported on the use of graphite nanoplatelets (38).

Recently, Novoselov *et al* reported the isolation of graphene by employing the technique of micromechanical cleavage, which involves mechanical exfoliation of small mesas of highly oriented pyrolitic graphite (39, 40). In recent years, the use of graphene as catalyst support has been also a topic of extensive research especially because of its interesting properties, which include excellent electronic and thermal conductivity, mechanical and thermal stability, and high surface area (as compared to graphite) (41, 42). However, in addition to the well-structured materials such as fullerene, carbon nanotubes, graphene and graphite there are many other forms of carbon material such as carbon black, graphite oxide, activated carbon, and carbon fibres in which graphene is the building block. These carbon materials have wide range of applications for example, carbon blacks find their use as catalyst supports in fuel cells, in car tires, and as fillers in polymers used in conductive packaging for electronic components. Similarly, graphene oxide, activated carbon, carbon fibre also find their application in catalyst support (43–52). However, theoretical studies on structural and chemical properties of these amorphous carbons have not yet been done in greater detail. In the following sections a brief discussion on the structural and chemical properties of these amorphous graphene-related carbon materials is presented.

1.2. Carbon black

Since the early 1900s, several models of the internal structure of carbon blacks have been proposed and in this regard, the review paper by Donnet provides an excellent

overview of some of these models (53). One of the first models of carbon blacks was proposed by Railey, which was based on the X-ray studies that basically corresponded

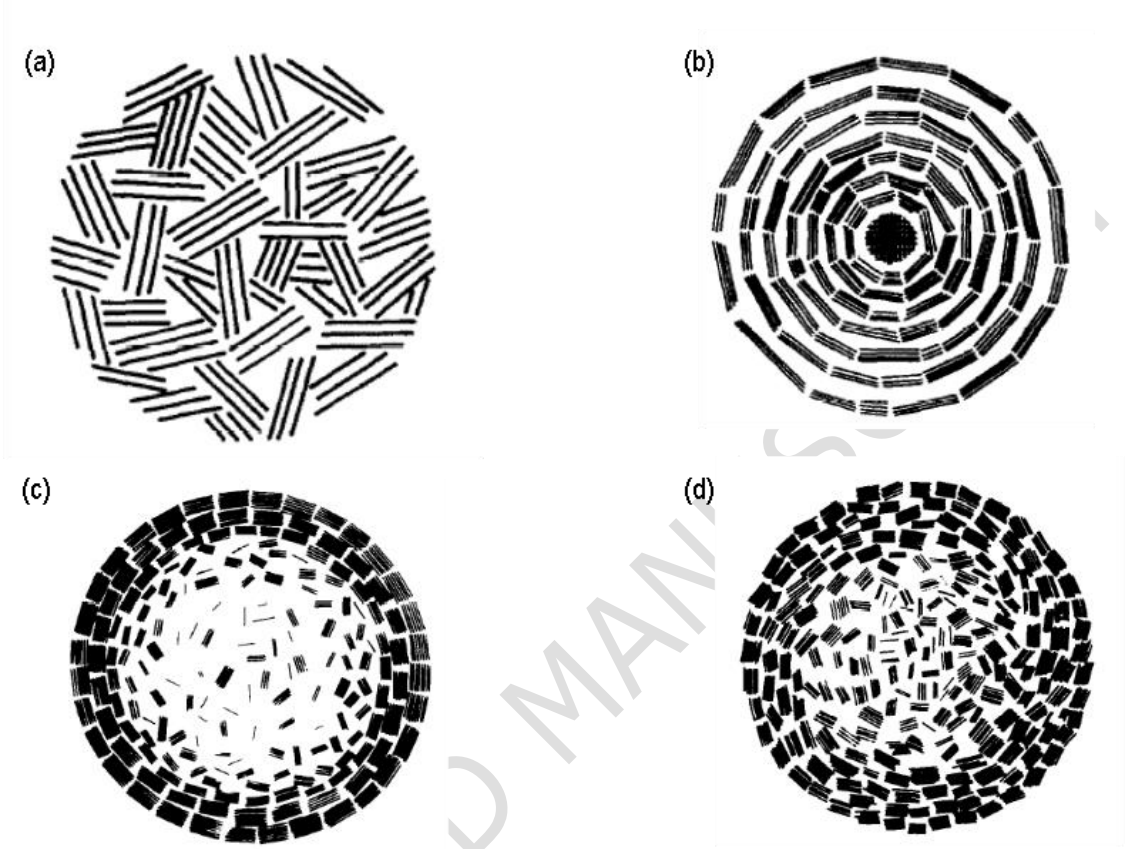

Figure 1. Carbon black models proposed by (a) Riley, (b) Bouland, (c) Shultz and (d) Hekman [Ref. J. B. Donnet, *Carbon.*, 1982, **20**, (4), 267].

to the average structure of particles reflecting the random distribution of crystallites and it represented the organized part of the carbon black particles [Figure 1(a)]. The improved models were proposed by Bouland [Figure 1 (b)] and Shultz [Figure 1(c)] in which the skin of the particle was believed to be more organized than its core. A more systematic model was proposed by Hekman [Figure 1 (d)], which was based on the x-ray and electron microscopy. In this model the skin of the particle was also proposed to be better organized than its randomly arranged crystallites in the core. Later, on the basis of results obtained from lattice fringe imaging technique, a more detailed

structure of carbon black was proposed by Heidenreich, Hess and Ban (54). In this model, (Figure 2) they also proposed that the ordering of the crystallite size and their ordering towards the centre of the particle are less than on the surface. According to all these models the commercial carbon blacks are made up of crystallites which are on average four graphite layer planes. The layers are roughly parallel and equidistant but do not exhibit the ABA stacking of hexagonal graphite. These graphite layer planes are referred to as basic structural units (BSU). The distance between the layers in the BSUs are larger than 3.35 Å. The size of these BSUs in the plane can differ between a few and 20 Å – 30 Å. If the samples become more amorphous, the number of stacked layers decrease until only one layer is left and simultaneously, the number of condensed rings in the plane also decreases (55). Recently Jäger *et al.* reported that the carbon black samples condensed in 10 mbar and 100 mbar Ar gas atmosphere were similar to the Riley model as shown in Figure 1 (a) (55). They further reported that the samples produced by them at 100 mbar Ar were close to the paracrystalline model (see Figure 3) where

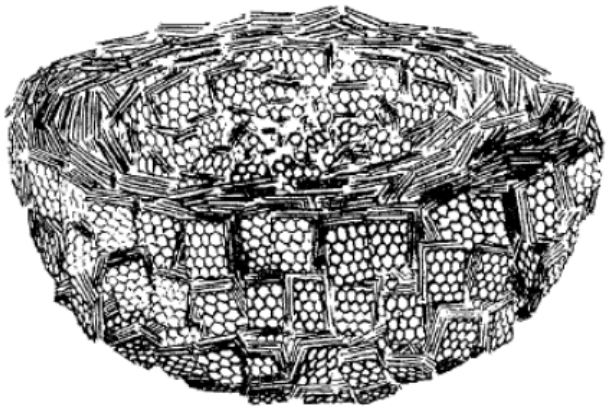

Figure 2. Model of carbon black based on lattice fringe imaging technique proposed by Heidenreich et al. [Ref. R. D. Heidenreich, W. M. Hess and L. L. Ban, *J. Appl. Crystallogr.*, 1968, **1**, (1), 1].

the curved and strongly distributed graphene layers are stacked together to form a particle.

In addition to the studies on the structural features of carbon black since the 1950s it is known that the surface of these particles have functional groups, which include hydroxyl, carboxyl, aldehydes, ketones, and quinones (53, 56, 57). Several researchers including Donnet *et al.*, Garten *et al*, Studebaker *et al*, Puri *et al* and Boehm *et al* in the 1950s and 60s independently arrived at this conclusion (53, 58–62). Since then various spectroscopic studies have also led to similar conclusions. For example, the recent FTIR spectral studies by Juan *et al* have shown that in the carbon black structures there are lots of aromatic C–C bonds and a large amount of oxygen containing organic functional groups (63). Other recent studies by Pantea *et al* have shown that in addition to oxygen containing groups, sulphur containing groups may be also present (43, 64).

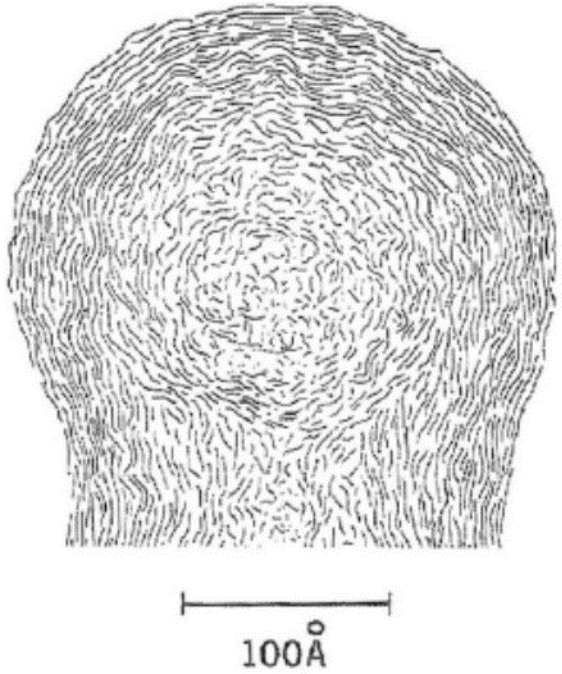

Figure 3. Paracrystalline model of carbon black (Ref. C. Jäger, T. Henning, R. Schlögl and O. Spillecke, *J. Non. Cryst. Solids*, 1999, **258**, 161)

1.3. Graphite Oxide

Preparation of graphite oxide was first reported in 1850, which was obtained by oxidizing graphite with $KClO_3/HNO_3$ (65, 66). Since then several other preparation methods of graphite oxides have been established and some of the most widely known methods are by Brodie, Staudenmaier and Hummers and Offeman and all these methods use strong oxidising agents such as $KClO_3$, $KMnO_4$ with HNO_3 (67–69). While the preparation methods for graphite oxide are well established, its structural features are still not fully understood. In this regard, several models have been proposed, which include:

1. *Ruess model*: In this model it was proposed that there are tertiary hydroxyl groups and ether bridges at 1,3 positions (67, 69, 70).
2. *Hoffman model*: In this model, the graphite oxides have enol- and keto-type functional groups with hydroxyls and ether bridges at the 1,3 positions (67, 70).
3. The Stuart and Briegleb model: In this model the graphite oxides are proposed to have carbonyl, hydroxyl and carbon-carbon double bonds (67, 69).

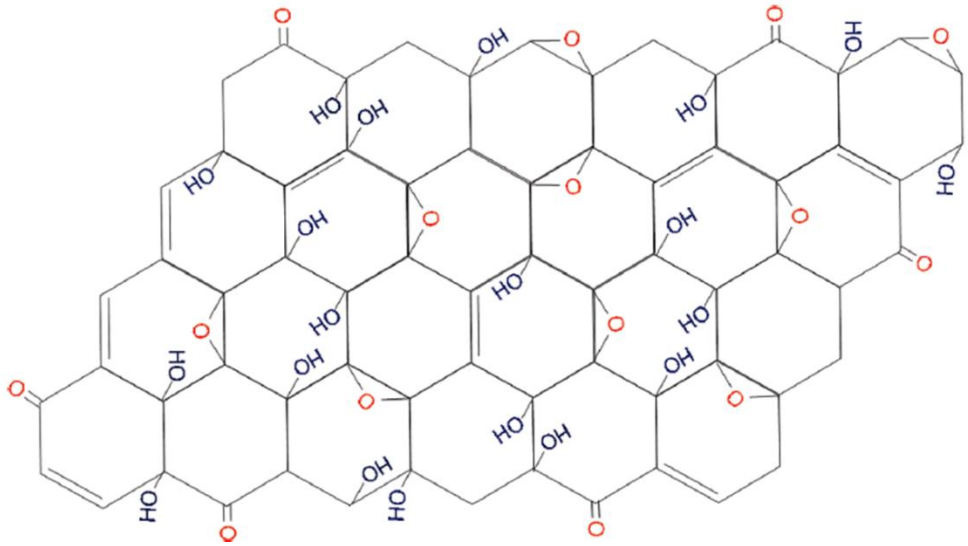

Figure 4. Graphite oxide model as proposed by Lee et al., which shows the presence of –O–, –OH and –C=O groups on the surface. (Ref. D. W. Lee, L. De Los Santos V., J. W. Seo, L. L. Felix, A. Bustamante D., J. M. Cole and C. H. W. Barnes, *J. Phys. Chem. B*, 2010, **114**, (17), 5723)

In another study, Lerf *et al* employed ^{13}C and ^{1}H NMR techniques to propose a newer structural model of graphite oxide, which consists of two kinds of regions *i.e.,* (a) aromatic regions with unoxidized benzene rings and (b) regions containing aliphatic six membered rings (71). In this model, the aromatic entities, double bonds and epoxide groups give rise to a nearly flat carbon grid and only the carbons attached to –OH groups are in a slightly distorted tetrahedral configuration, resulting in some wrinkling of the layers. It was further reported that the functional groups lie above and below the carbon grid forming a layer of oxygen atoms of variable concentration. Like graphite itself, graphite oxide has a layered structure, but its carbon layers contain large quantities of functional groups, mainly –OH and –CHO (72). We note that modifications of graphite oxide with soft donor atoms of sulphur have been also reported by Talanov *et al* (73). Further to this, recent studies on the graphite oxide structure, using various microscopy and spectroscopic techniques, proposed a new model of GO, which indicates the presence of –O–, –OH and –C=O groups on the surface. In these models, the two neighbouring –OH groups are located on opposite sites in order to reduce the electrostatic repulsions in between them and for the same reason the –OH groups are located away from each other. The epoxy and ketone groups are also away from the –OH groups (See Figure 4)(74). Additionally, the presence of five- and six-membered-ring lactols has also been proposed (75).

1.4. Activated Carbon

The surface structure of activated carbon is highly complex and depends on the raw material used, and method adopted for their production. It is believed that activated

carbon generally consists of graphite crystallites with highly disordered, irregular, rough and heterogeneous surfaces (76). There are many experimental studies, which have reported the surface chemistry of activated carbon and methods to evaluate it (77, 78). The infrared study on the surface structure of activated carbons has indicated the presence of oxygen-containing organic functional groups such as C=O in lactones and carboxylic anhydrides, quinine and aceto-enol groups and C-O group in ethers, lactones, phenols and carboxylic anhydrides (79). The structure of activated carbons is still not fully understood.

1.5. Carbon Fibres

Carbon fibres (CF) are generally in the range of 5–50 μm, which are commercially produced by converting a carbonaceous precursor into fibre. The Polyacrylonitrile-based (PAN-based) and mesophase pitch-based CFs are two of the most dominant CFs (80). Several studies have shown that the PAN-based CFs have extensively folded and interlinked tubostratic layers (*i.e.,* the sheets of carbon are haphazardly folded and crumbled together) with interlayer spacing larger than those of graphite (80, 81). Mesophase pitch-based carbon fibres on the other hand may have radial (graphene planes radiating out from the centre of the fibre), random (with random orientation of graphitic planes) or onion or quasi-onion like transverse microstructures (80, 82). The mesophase-pitch based CFs usually have a larger diameter (10 – 15 μm) as compared to the PAN-based CFs (5 – 7 μm) (81). In addition to understanding the detailed structural features of carbon fibre there have also been numerous experimental studies on the characterisation of the surficial reactive functional groups in CFs (83–85). In

this regard, the studies by Szabó *et al.* showed that CFs consist of mainly –OH groups (~97%) and small amounts of $–NH_2$ (~2.7%) and –COOH (~0.3%) groups (85).

1.6. Soot

Finally, we briefly comment on the structural and chemical features of soot, as carbon black is sometimes confused with soot even though they are very different materials (86). While carbon blacks are made under closely controlled conditions, soot is produced as a byproduct of incomplete combustion of a hydrocarbon or pyrolysis (87, 88). The gas-phase soot contains polycyclic aromatic hydrocarbons (PAHs). It has been found that soot is made of spherical-like particles with diameters in the 20- to 50-nm range. These particles are composed of graphite-type microcrystallites layers which are concentrically arranged in an onionlike structure. The graphitic layers are found to contain surface OH and C=O groups (89).

2. A brief discussion on density functional theory

After having briefly reviewed the structural and chemical features of some interesting ordered and amorphous carbon materials, in the next section we present an outline of the density functional theory.

2.1. The Hohenberg-Kohn Theorem

In 1964, Pierre Hohenberg and Walter Kohn proposed and proved that for a nondegenerate ground state all the ground state electronic properties are determined

by the ground state electron density (ρ_0), which could be mathematically represented as:(90, 91)

$$\rho_0(\mathbf{r}) \rightarrow v_{ext} \rightarrow \Psi_0 \rightarrow \text{all properties} \quad [1]$$

Here, v_{ext} is the Coulomb potential energy between electrons and the nuclei, and Ψ_0 is a unique ground state wave function(92). The electron density is dependent only on three spatial variables ($\mathbf{r}$) whereas, the wave function depends on 3*N* variables for a system of *N* electrons.

Thus, the ground state energy can be written as a functional of the ground state electron density,

$$E_0 = E_{v_{ext}}[\rho_0] = \bar{T}[\rho_0] + \bar{V}_{ne}[\rho_0] + \bar{V}_{ee}[\rho_0]. \quad [2]$$

Here, $\bar{T}, \bar{V}_{ne}$ and $\bar{V}_{ee}$ are the average kinetic energy, potential energy due to nucleus-electron and electron-electron interactions, respectively. The $\bar{V}_{ne}$ term in equation [2] can be further written as:

$$\bar{V}_{ne} = \langle\psi_0| \sum_{i=1}^{n} v(\boldsymbol{r}_i) |\psi_0\rangle = \int \rho_0(\mathbf{r}) v(\mathbf{r})\, d\mathbf{r} \quad [3]$$

where, $v(\boldsymbol{r}_i)$ is the nuclear-electron potential energy for the i^{th} electron.

Combining equations [2] and [3] yields

$$E_0 = E_{v_{ext}}[\rho_0] = \bar{T}[\rho_0] + \int \rho_0(\mathbf{r}) v(\mathbf{r})\, d\mathbf{r} + \bar{V}_{ee}[\rho_0]. \quad [4]$$

The term $\bar{T}[\rho_0] + \bar{V}_{ee}[\rho_0]$ in equation [4] is unknown.

In the ***Hohenberg-Kohn variational theorem***, Hohenberg and Kohn further proved that, the true ground state electron density minimizes the energy functional $E_v[\rho_{tr}]$, where ρ_{tr} is the trial density function that satisfies $\int \rho_{tr}(\mathbf{r})d\mathbf{r} = N$ and $\rho_{tr} \geq 0$ for all **r** and the inequality $E_0 \leq E_v[\rho_{tr}]$ holds where, E_v is the energy functional in the equation (4). Hohenberg and Kohn proved their theorems only for nondegenerate ground states and later Levy proved the theorems for degenerate ground states(93).

While the Hohenberg-Kohn theorem tells us that if we know the ground-state electron density $\rho(\mathbf{r})$, we can determine the ground state wave function, it however does not tell how to calculate E_0 from ρ_0. It also does not tell how to obtain ρ_0 without finding the wavefunction.(90),(94) In 1965 Kohn and Sham revisited this problem, which is briefly outlined below.

2.2 The Kohn-Sham Method

Kohn and Sham considered a fictitious system of *N* non-interacting electrons, which experiences an external potential energy $v_s(\mathbf{r}_i)$ (index *s* is reserved here for the fictitious systems) (94). It was further assumed that the electron density of this reference system $\rho_s(\mathbf{r})$ is equal to the exact ground state electron density $\rho_0(\mathbf{r})$ of the system of *N* interacting electron system under consideration (molecule). The Hamiltonian of this system is given by:

$$\hat{H}_s = \sum_{i=1}^{n}\left[-\frac{1}{2}\boldsymbol{\nabla}^2 + v_s(\boldsymbol{r_i})\right] \equiv \sum_{i=1}^{n}\hat{h}_i^{KS} \quad (5)$$

where, $\hat{h}_i^{KS}$ is the one-electron Kohn-Sham Hamiltonian for the fictitious system (Kohn-Sham Hamiltonian). Additionally, since this system consists of noninteracting electrons, the ground state wave function $\psi_{s,0}$ is the antisymmetrized product (using

the Slater determinant) of all the lowest energy one-electron spin-orbitals, which are the product of one-electron spatial orbital and a one-electron spin function. Further to this, they defined the difference between the kinetic energy of the interacting N-electron system and that of the fictitious system as:

$$\Delta\bar{T}[\rho] \equiv \bar{T}[\rho_0] - \bar{T}_s[\rho], \quad [6]$$

where, $\bar{T}[\rho_0]$ and $\bar{T}_s[\rho]$ are the average electronic kinetic energies of the interacting *N* electron system and the fictitious noninteracting *N* electron system respectively. Similarly, the quantum mechanical many-body electron-electron interaction energy minus the classical one can be represented as:

$$\Delta\bar{V}_{ee}[\rho] \equiv \bar{V}_{ee}[\rho_0] - \frac{1}{2}\iint \frac{\rho(\mathbf{r}_1)\rho(\mathbf{r}_2)}{r_{12}} d\mathbf{r}_1 d\mathbf{r}_2. \quad [7]$$

Here the term ½ is added so that the repulsion energy between the charges is not counted twice.

For simplicity, we can omit subscript 0 from ρ and by rearranging and substituting equation [6] and [7] in equation [4] we have:

$$E_{v_{ext}}[\rho_0] = \Delta\bar{T}[\rho] + \bar{T}_s[\rho] + \int \rho(\mathbf{r}) v(\mathbf{r})\, d\mathbf{r} + \Delta\bar{V}_{ee}[\rho] + \frac{1}{2}\iint \frac{\rho(\mathbf{r}_1)\rho(\mathbf{r}_2)}{r_{12}} d\mathbf{r}_1 d\mathbf{r}_2 , \quad [8]$$

which can be also rewritten as

$$E_{v_{ext}}[\rho_0] = \bar{T}_s[\rho] + \int \rho(\mathbf{r}) v(\mathbf{r}) d\mathbf{r} + \frac{1}{2}\iint \frac{\rho(\mathbf{r_1})\rho(\mathbf{r_2})}{r_{12}} d\mathbf{r}_1 d\mathbf{r}_2 + E_{xc}[\rho] , \quad [9]$$

where,

$$E_{xc}[\rho] = \Delta\bar{T}[\rho] + \Delta\bar{V}_{ee}[\rho]. \quad [10]$$

which is referred to as the *exchange-correlation (xc) energy functional* (94) and it is responsible for all the many-body electron-electron interaction. The term E_{xc} can be also written as:

$$E_{xc} = E_x + E_c \ , \qquad [11]$$

where E_x and E_c are exchange and correlation energy respectively.

We note that even though the xc energy is a small part of the total energy of a typical system it plays the vital role in binding atoms together and therefore, Perdew coined it as "nature's glue" (95). This quantum mechanical phenomenon arises as electrons move in such a way to avoid one another, which in turn, lowers the expectation value of the electron-electron Coulomb interaction. The exchange energy in the xc functional (equation [11]) is a consequence of the system obeying the Pauli principle and is free from the spurious self-interaction of an electron, when the exact Fock exchange is used. The correlation energy ($E_c = E_{xc} - E_x$) should account for the remaining effects of spatial and spin correlation in the many electron system.

Table 1. Some popular examples of exchange and correlation functionals.

Types of exchange and correlation functionals	Typical examples
Local density approximation (LDA)	VWN (96), PZ81 (97), PW (98)
Generalized-gradient approximation (GGA)	PW91(98), PBE(99), RPBE(100), RevPBE(101), PBE_{Sol}(102)

van der Waals density functional (vdW-DF)	vdW-DF(103), vdW-DF2 (104), optB88-vdW(105), rev-vdW-DF2(106)
Meta-GGA	M06-L(107)(108), TPSS (109), Rev-TPSS (110)
Hybrid functionals	B3LYP(111), O3LYP (112), HSE03(113), HSE06(114), PBE0(115) CAM-B3LYP(116), LC-ωHPBE(117)

Some of the popular exchange and correlation functionals are summarised in Table 1, which is not a complete list of all the exchange and correlation functionals currently available.

3. Adsorption of transition metals atoms

3.1 Adsorption of transition metal catalyst on single and multi-layered graphene

The earlier theoretical studies on the adsorption of transition metal (TM) adatoms on carbon materials were mainly reported on a single layer of sp^2 hybridised carbon support with some reports on a few layers of graphene and these studies were mainly focused on structure, bonding, magnetic properties of the adsorbed TMs on graphene and their migration to the high symmetry sites (118). Duffy *et al.* for example, used the linear combination of atomic-orbitals-approach as implemented in DMol package to study the effect of the surface on the 3*d* TM adatoms and dimers on a cluster model

of graphite.(119),(120, 121). In their calculation they used the local spin density approximation using the Vosko-Wilk-Nusair (aka VWN) exchange and correlation functional (96). They reported that the preferable adsorption sites of Sc, Ti, Cr, and Mn are above the C-atoms while Fe, Co and Ni prefer over the rings. Due to the hybridization between these metals with the π-orbitals of graphite there is a small electron transfer. It was also seen that the total magnetic moments are higher for Sc, Ti and V by 1 μ_B than the free atom and lower by 2 μ_B for Fe, Co and Ni, while Cr and Mn have reversed their free atom values. To understand this behaviour, they considered the local density of states of the Fe/graphite (with C_{6v} symmetry: Fe stable over the hole-position) and V/graphite (with C_{3v} symmetry: V stable over-atom position) systems. In the Fe/graphite system, the molecular orbitals (MOs) mainly comprise 3*d* and 4*s* orbitals and a small admixture of 4*p* orbitals. These molecular orbitals are labelled by the C_{6v} group *i.e.*, a_1, a_2, b_1, b_2, e_1 and e_2. However, only the a_1, e_1 and e_2 orbitals have metallic as well as C π-orbital components. A careful analysis of these orbitals showed that the adsorbed atom has the tendency to shift the 4*s* orbital energy up with respect to the 3*d* orbitals meaning an electron configuration of $3d^{n+2}4s^0$ is preferred over $3d^n4s^2$ where $1 \leq n \leq 8$ of the elements under consideration (note that Cr has an electron configuration of $3d^5 4s^1$ due to half-filled electron configuration being more stable). From such analysis they were able to explain the reduction of the atomic

spin moment by $2\mu_B$ in Fe. Similar analyses were done on V/graphite system, which showed that there is also a tendency for increased population of 3*d* related MOs but due to its enhanced hybridization with the graphite surface this effect is reduced, which leads to an increase in the spin moment by $1\mu_B$. In another study, Valencia *et. al*. performed periodic spin polarised density functional theory calculations using a projector-augmented wave scheme (PAW), and the PW91 exchange and correlation

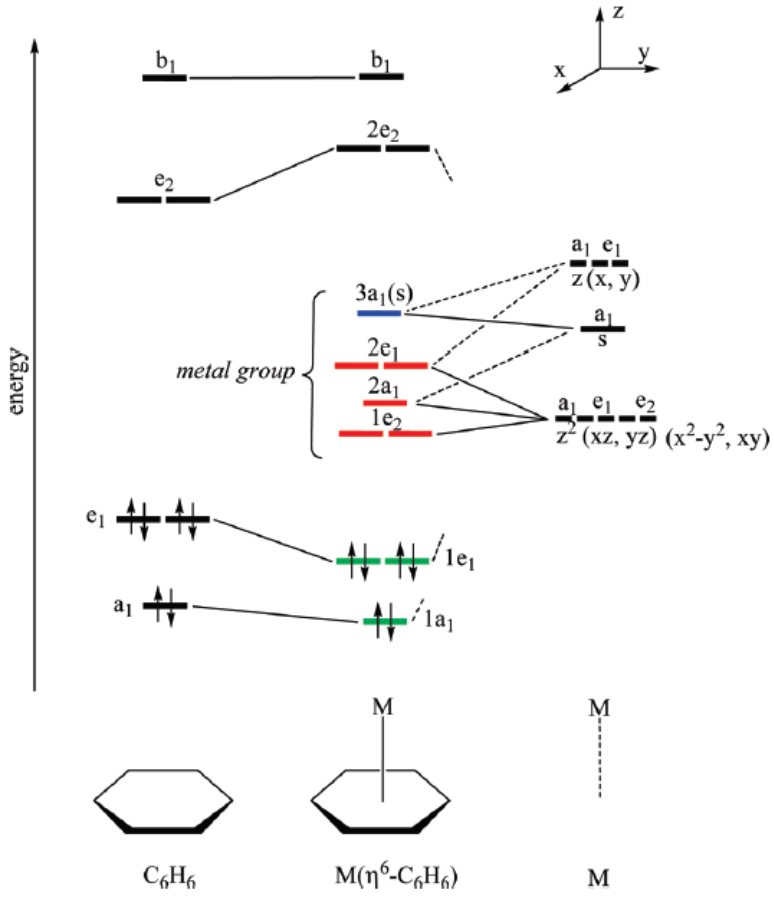

Figure 5. Qualitative MO interaction diagram for M+C_6H_6. Only the six π MOs of benzene were considered. Labels for the MOs are indicated within the C_{6v} symmetry point group. Metal valence electrons are not shown (Ref: Valencia *et al*. J. Phys. Chem. C, 2010, 114, 14141).

functional as implemented in the VASP code to explore the trends in adsorption of the 3*d* transition metal atoms on graphene.(122) They found that Sc, Ti, Fe and Co could

remain isolated on the graphene surface but other metals in this series may diffuse with a possibility to form aggregates. They employed density of states and Bader charge analysis to explain the observed trends. Another interesting aspect of this study was the use of the organo-metallic M(η^6-C_6H_6) molecular orbitals to bridge the language used to describe molecular states and that used to describe solid states. **Figure 5**, shows the qualitative interaction orbital diagram for the M(η^6-C_6H_6) C_{6v} system using Hückel calculations by means of CACAO.(123–126) This simplified MO diagram shows six 2π-orbitals of benzene and the valence orbitals of the 3*d* TM atom and as described above, these orbitals are labelled by the C_{6v} group. Of the six 2π-orbitals, three with a_1 and e_1 symmetries are occupied, which interacts with the 4*s* and 3*d* orbitals of similar symmetries giving three bonding orbitals mainly localised on the benzene participating in the M-C bonds directing downward. The three antibonding orbitals, which remain unoccupied are mainly localised on the metal 4*s* and 3*d* orbitals and directed upward. The metallic group orbitals are shown in the centre of the interaction diagram and they are formed of $1e_2$ (from mixing of $3d_{x^2-y^2}$ and $3d_{xy}$ orbitals, with antibonding π^*_{CC}orbitals of benzene participating in metal-carbon δ bonding), $2a_1$ (from mixing of 4*s*, $3d_{z^2}$, $4p_z$ orbitals and the in-phase π_{CC} MO, which leads to a nonbonding σ MO), $2e_1$ (formed by mixing of $3d_{yz}$, $4p_x$ and $4p_y$ orbitals interacting with the bonding π_{CC}) and $3a_1$ (derived mainly from the metal 4*s* orbital). They employed this qualitative M(η^6-C_6H_6) MO description along with the calculated partial density of states for the periodic M@graphene to show that the energy levels follow a global order *i.e.,* $1e_2 \sim 2a_1 < 2e_1 < 3a_1$ and they used this scheme to clarify the observed trends on chemisorption of 3*d* TM with an exception of half-filled Cr and

Mn and fully filled Cu 3*d* atoms, which physisorb on the graphitic surface. Further to this, they used qualitative molecular orbital diagrams and charge transfer considerations to explain the trends observed in computed magnetism. They also concluded that Sc, Ti, Fe and Co are stable as isolated atoms on the graphitic surface and other metals diffuse to eventually form aggregates. In another interesting study Nakada *et al*. reported the adsorption and migration energies of adatom with atomic numbers 1 - 83 on graphene at the LDA level of theory using the PAW method as implemented in VASP.(127) In this study they reported that the transition metal elements mainly adsorb on the hollow sites. They noted that the adsorption types can be of two types *i.e.,* with fixed adsorption and those with no fixed sites. For the systems with no fixed adsorption sites they estimated the migration energy barrier as 0.5 eV where, the minimum limit of the migration energy was obtained by taking the difference between the adsorption energies for each site. They concluded that for metal-graphene junctions in addition to the adsorption energies the migration energy plays an important role. Recent studies by Manadé *et al*. also reported a systematic study on the adsorption of 3*d*, 4*d* and 5*d* TM adsorbed on graphene. In this study they also concluded that TMs prefer the hollow sites when chemisorbed. However, if they are physisorbed for example, in the case of d^5 and d^{10} configuration, then they prefer the bridge or the top sites. Their study showed that inclusion of dispersive forces simply increases the adsorption energies of the TM by ~0.35eV. They also reported the electron transfer behaviour of the TMs and found that it decays along the series because of the increase in electronegativity.(128)

In addition to the adsorption of transition metals on a single layer graphene, studies on the adsorption of metal adatoms have been reported on bilayer and trilayer graphene.(129),(130),(131),(132) For example, Hardcastle *et al.* employed plane-wave density functional theory to investigate the adsorption properties of Au, Cr and Al atoms on the armchair and zigzag sites of monolayer graphene and on the adsorption sites of single, bi and tri layer graphene. They investigated the adatom mobility on the pristine substrates.(132),(133) They used the CASTEP code with PBE exchange and correlation functional in conjunction with Tkatchenko-Scheffler van der Waals correction scheme (134). In this study they concluded that the graphene sublayers make a significant contribution to the total binding energy of the adatom and the adatoms are extremely mobile on graphene at room temperature. In the recent years, the trends of theoretical studies on the interaction of TMs on graphene, have moved towards exploring the interaction of more realistic metal nanoparticles on graphene(135, 136). For example, Engel *et al*. recently systematically studied the electronic properties of Au clusters on graphene using DFT-D+U(135). Further to this, the interactions of molecules for example, NO_2, H_2S, and glucose on TM atoms and clusters supported on pristine graphene have been also reported (137),(138),(139).

3.2 Adsorption of transition metal catalyst on graphene with vacancies

Graphene can display single and/or multiple vacancies but it is worth-mentioning that the filling of such a vacancy may occur due to the reservoir of loose carbon atoms readily available nearby these vacancies (140),(141). The single vacancy refers to a missing C-atom from the lattice and the double vacancy can be created by combining two single vacancies or by removing two neighbouring C-atoms. Double vacancies may

result in different types of configuration *i.e.*, two pentagons and one octagon (5-8-5), three pentagons and three heptagons (555-777) and four pentagons, one hexagon and four heptagons (555-6-7777) (140). Therefore, in addition to the interaction of transition metals on pristine graphene, studies on graphene with single and double vacancies have been also reported, which is not only interesting from the catalysis point of view but also from the context of spintronics and Kondo physics (142). Krasheninnikov *et al*. for example, presented a density functional theory study on the structure, bonding and magnetic properties of the first transition metal series, Pt and Au on the single and double vacancies of single graphene sheets (142). They found that on the single vacancies (SV), all the metal atoms form covalent bonds with the under-coordinated C atoms and as the atomic radii of TMs are larger than carbon, the metal atom bulges out of the graphene plane. The TM-C bond lengths were seen to decrease from Sc to Fe due to the decrease of the TM radii and then it increases as bonding becomes weaker. The calculated binding energies of the TMs on the single vacancies were typically about -7 eV with an exception of fully filled *d*-shell elements such as Cu and Zn. They further noted that single vacancy complexes are magnetic for V, Cr, Mn, Co and Cu and nonmagnetic for Fe and Ni. On the other hand the transition metals on double vacancies all the TMs from V to Co are magnetic, which is related to the fact that on double vacancies due to the larger "hole" the interactions of the TMs are weak and therefore, the complexes are in higher spin states. In another study Krasheninnikov *et al*. using strain fields, further demonstrated that metal atoms have high affinity to the non-perfect and strained regions of the graphene with defects (143). In this work they visualised the strain fields as the difference between the bond

lengths between the graphene sheet with and without defects, which suggested that all vacancies result in strain fields in the vicinity of the defects in the range of 2-3 nm or even more. In 2013, Robertson *et al*. used aberration corrected transmission electron microscopy (ACTEM), high resolution (HR-) TEM, electron microscopy and DFT to show that single Fe atoms can be trapped on the single and double vacancies of graphene, forming covalent bonds and causing significant displacement, up to 0.5 Å, of the surrounding carbon atoms. They further reported that Fe on such vacancies are more stable than when they are incorporated into the graphene edge.

In recent years, theoretical studies have moved towards understanding the interaction of small TM clusters on the single and double vacancies of graphene. In this regard, Sen *et al*. investigated the stability and electronic properties of Pd_n (n = 1–5) clusters on different types of double vacancies mentioned above using DFT and molecular dynamic simulations (144). Their study revealed that the adsorption of Pd_4 clusters on the defect bridge site of double vacancy of (555-777) is favourable, which they concluded is because of the hybridization between C *2p* and Pd 4*d* and 5*s* orbitals and higher charge transfer to the graphene sheet. Further to this, the latest studies in this area are focused on understanding the interaction of molecules on TM clusters adsorbed onto the graphene lattice vacancies. For example, Hamamoto *et al*. used DFT to demonstrate that the local electronic properties of CO adsorbed on Pt_4 clusters supported on graphene with 1 to 4 vacancies are remarkably altered due to its interaction with the dangling bonds of carbon atoms in the defect sites (145).

3.3 Adsorption of Transition metal catalysts on doped graphene

The introduction of heteroatoms such as N and B into the carbon framework of graphene can be used to tailor the electronic and local geometrical properties of graphene for applications in catalysis.(146)-(152) The substitution of N (n-type doping) in the graphene lattice usually leads to four common bonding configurations, which include (i) quaternary N (obtained by substituting the C-atoms of the hexagonal ring by the N-atoms), (ii) pyrrolic N (obtained by N-atoms due to the bonding on the five-membered rings as in pyrrole), (iii) pyrazolic N (obtained by the insertion of an aromatic N_2 moiety in a five-membered ring as in pyrazole) and (iv) pyridinic N (obtained by substitution of the N-atoms at the defect sites or on the edge of graphene as in pyridine) (146),(153),(154). Similarly, it has been shown that doping with boron (p-type doping) or more complex functional groups such as boronic esters and boronic acids can be also done on graphene (155). Such incorporation of dopant atoms leads to significant alteration of the electronic properties of graphene for example, Zhang *et al*. theoretically showed that substitution of N on the graphene framework introduces asymmetric spin density and atomic charge density making it favourable to oxygen reduction reactions (156). Recently, reports on doping of graphene with Be, S, Si, and P have been also made (157),(158). It is worth mentioning that doping on graphene can be also achieved by electron exchange between adsorbed species on graphene surfaces (148).

It has been now shown that the durability and activity of transition metal catalysts such as Pt increases significantly on N-doped carbon supports (159). In this regard, numerous theoretical studies have also been performed for example, Groves *et al*. used DFT as implemented in the GAUSSIAN03 package on 42 C-atom cluster models

to calculate the binding energy between N-doped graphene structure and Pt adatoms in order to explore the molecular orbital and natural bonding orbital data (160). They showed that N-doping increases the binding energy of Pt to the substrate and the binding energy increases if the N-atoms are closer to the C-atom bonded directly to the Pt adatom. In another study Zhou *et al*. employed the DMol^3 code to study the effect of N and B doping on the stability of defective graphene supported Ni_n (n= 1 – 6) clusters (2). They found that the binding energies of these clusters on doped defective graphene were higher than on pristine graphene meaning the stability of Ni clusters were further improved. It was also seen that Ni_n clusters were more stable on the B-doped defective graphene than the N-doped once. The probable reason for this was attributed to the fact that B heteroatoms promote stronger hybridization between C-atoms and Ni-atoms. Another interesting study by Kropp *et al*. also found that N doping resulted in increased binding energies of transition metals (161). These studies clearly suggested that N and B-doped graphene can be good catalyst support. We note that in recent years there have also been some studies in which the adsorption of small gas molecules on transition metal doped graphene have been reported (162).

3.4. Adsorption of Transition metal catalysts on amorphous carbon.

Theoretical studies on the geometrical and electronic properties of graphene (mainly graphene nanoflake cluster models (GNFs)) with organic functional groups (OFGs) to model the basic structural units of carbon black, graphene oxide, activated carbon and soot have been reported (8, 163–167). For example, Efremenko *et al* reported the adsorption properties of phenol on activated carbon, Hamad *et al.* reported the adsorption of water on soot particles and we have also investigated the detailed

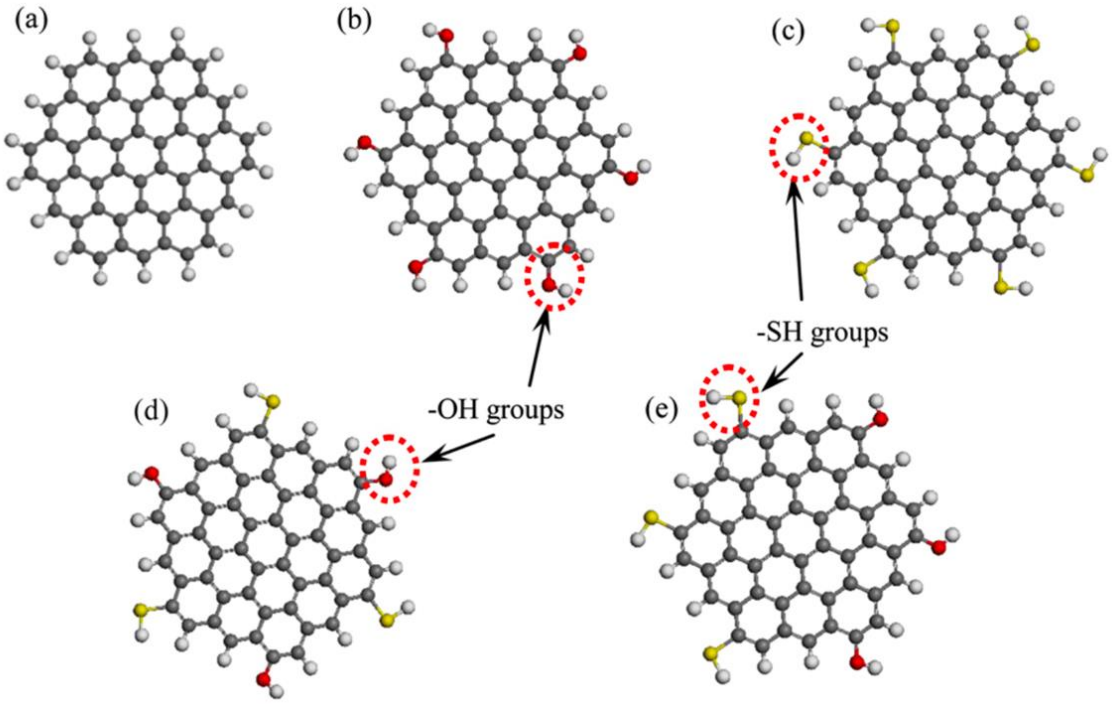

Figure 6. (a) Pristine graphene (G) model saturated with H-atoms, (b) G(OH), (c) G(SH), (d) G(OS-C_{3h}) and G(OS-C_s) (Ref. A. Chutia, F. Cimpoesu, H. Tsuboi and A. Miyamoto, *Chem. Phys. Lett.*, 2011, **503**, (1–3), 91)

electronic properties of graphene nanoflakes with OFGs to mimic the BSUs of amorphous carbon materials discussed earlier in section 1 with various shapes and sizes (76, 89, 163–165). In this regard, we investigated the influence of orientation and stacking patterns of the model BSUs on the electronic properties. In these models, the oxygen containing OFGs such as –OH, –CHO, and –COOH were decorated on the periphery of the GNF models. In one of these studies we used –OH and –SH groups to understand the effect of chemical constitution of these materials (Figure 6). The models constituted of pristine GNF models (referred to as G in Figure 6(a)), with only –OH groups (*i.e.*, G(OH)), with only –SH groups (*i.e.,* G(SH)) and models with mixed –OH and –SH groups (*i.e.*,G(OS-C_{3h}) and G(OS-C_s); C_{3h} and C_s refers to the symmetry of the models). Additional studies on the effect of different stacking conformations with

two, three and four layers of G(OH) and G(SH) models on the electronic properties were undertaken (see Figure 7). From these studies it was seen that in the fully relaxed geometries, the CSH angles (due to the –S…HS– bonds) were closer to 90° when compared with the COH angles (due to the –O…HO– bonds), which was related to different hybridization abilities of the O and S-atoms and due to the charge-charge interaction in O…H and charge-quadrupole interaction in S…H. Further to this, it was concluded that by substitution of different OFGs and by using different stacking patterns (such as AAA or ABA) the electronic properties of these systems could be significantly altered. Based on these studies, we also investigated the adsorption properties of Pt-adatom and Pt_4 cluster on GNFs with varying concentration of hydroxyl groups (*f*-GNFs) (8). In this study, based on the DFT results it was proposed that the

loading of Pt catalyst on carbon supports could be engineered by controlling the concentration of oxygen containing OFGs. In addition to the studies on decorating graphene with oxygen containing OFGs there are several studies in which the O-doped graphene have been used to investigate the adsorption properties of transition metal clusters, which include Pt_4, and Pt_3M (M=Sc, Ti, V, Cr, Mn, Fe, Co and Ni) (168, 169). In one of these studies, Cui *et al* reported that Pt_3Ni supported on the O-doped

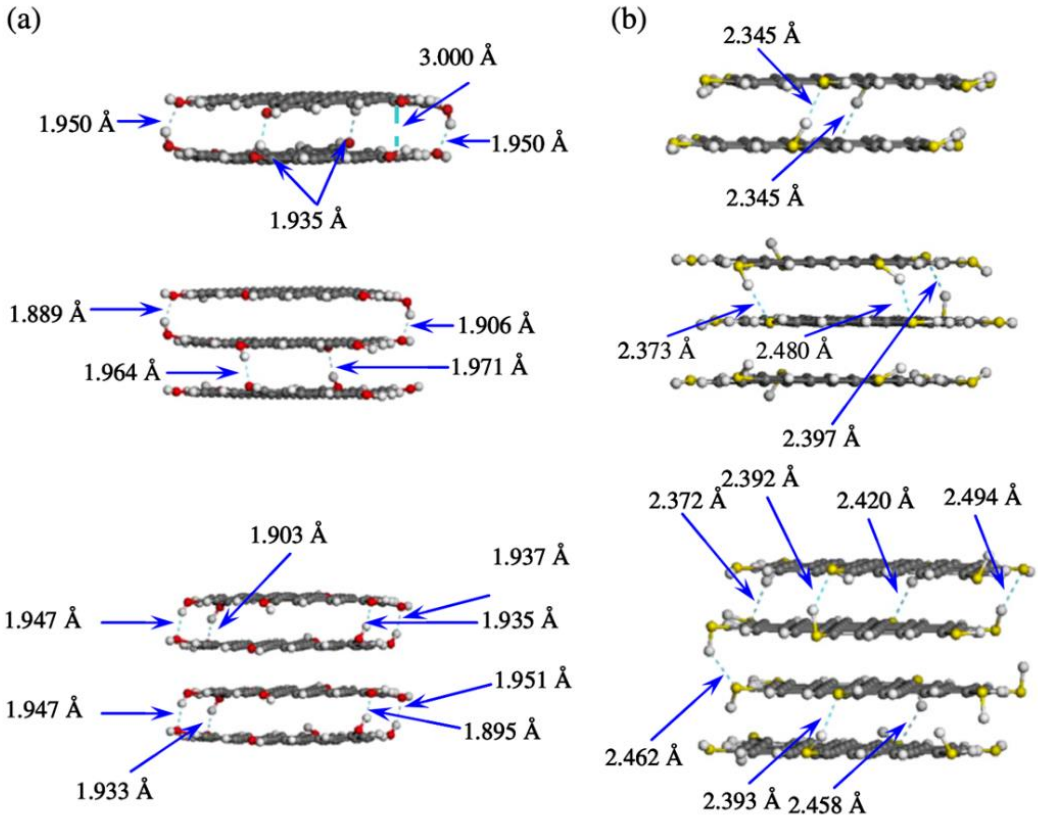

Figure 7. Optimised geometries of (a) G(OH) and (b) G(SH) (Ref. A. Chutia, F. Cimpoesu, H. Tsuboi and A. Miyamoto, *Chem. Phys. Lett.*, 2011, **503**, (1–3), 91)

graphene exhibit enhanced catalytic performance (169). In some recent work, more complex studies of transition metal adsorption on the OH decorated N-doped graphene have been reported. For example, Sahoo *et al* used transmission electron microscope (TEM), high resolution TEM (HRTEM), hard X-ray photoelectron spectroscopy

(HAXPES), combined with DFT calculations to report the charge transfer of Pd catalyst to pyrrolic-N doped reduced graphene oxide (NRGO) (170). In this study, they showed that strong bond between Pd and pyrrolic-fraction of the N-moieties can be formed, which can be further strengthened by the presence of oxygen containing functional groups. This study further reported that the charge-transfer from the Pd 3*d*-orbitals to the 2*p*-orbitals of C, N and O of NRGO results in high oxygen reduction reaction. In another recent study Rout *et al* synthesised highly active and well-defined Au-Cu nanoparticles supported on reduced graphene oxide(171). These nanoparticles were then characterised using various techniques, which include UV-vis, XRD, HRTEM, STEM Raman and XPS. They found that Au_3Cu_1 bimetallic clusters exhibited superior catalytic activity. In this study, they used density functional theory on cluster models of reduced graphene oxide to clarify the reasons for the high catalytic activity of these nanoparticles. They concluded that efficient adsorption of the highly dispersed Au_3Cu_1 on reduced graphene oxide led to the enhanced catalytic activity.

As we can see from the above studies, the models on the amorphous carbons such carbon black, graphene oxide, activated carbon, and soot are based on a single layer of graphene. This is especially because of the complexity in modelling these systems. However, there are some interesting studies made towards modelling of complex amorphous carbons. For example, recently Caro *et al* reported a systematic study in which they combined machine learning and DFT to theoretically understand the surface chemistry of amorphous carbons (172). In another study Ranganathan *et al.* employed molecular dynamics simulation to produce models of amorphous carbons (173). Clearly, more research in this area is required to reproduce as realistic models of

amorphous carbons as those of the experiments and to understand the interaction between these catalyst supports and catalysts to design novel and efficient catalysts.

4. Concluding remarks and future direction

In this short review, we presented a discussion on the structural and chemical features of graphene related carbon materials, which are widely used as catalyst supports. We summarised that, so far numerous theoretical studies have been done on the adsorption properties of transition metal adatoms, and clusters on graphene and related systems. The current trend of these studies is moving towards modelling more and more realistic transition metal nanoparticles interacting with graphene. Most of these theoretical studies are however done on pristine and/or modified graphene models. Clearly, more theoretical research is required in this area to reproduce realistic models of amorphous carbon supports to complement the models reported in the experimental studies to further our understanding on the interaction between catalyst and catalyst supports to design novel and efficient catalysts. Here, we reviewed some of the important studies which employed density functional theory, however, to gain deeper understanding of the structure property relationship of these industrially important carbon materials and their interaction with catalysts, multiscale modelling will be required. Artificial intelligence and machine learning tools will be particularly beneficial in this pursuit.

Acknowledgement: We thank Dr. Ikutaro Hamada for his helpful discussion during the preparation of the manuscript. We also thank Cirrus UK national Tier-2 Service at EPCC (funded by University of Edinburgh and EPSRC (EP/P020267/1)), Athena at HPC

Midlands+ (Funded by EPSRC, EP/P020232/1), and ARCHER2 (via Materials Chemistry Consortium and EPSRC (EP/L000202)) and Supercomputer Wales.

References

1. B. C. S. Keith J. Laidler, John H. Meiser, 'Physical Chemistry', 4th Ed., Houghton Mifflin, Boston, New York, 2003

2. X. Zhou, W. Chu, W. Sun, Y. Zhou and Y. Xue, *Comput. Theor. Chem.*, 2017, **1120**, 8 LINK https://doi.org/10.1016/j.comptc.2017.09.011

3. J. Paier, C. Penschke and J. Sauer, *Chem. Rev.*, 2013, **113**, (6), 3949 LINK https://doi.org/10.1021/cr3004949

4. A. Chutia, I. P. Silverwood, M. R. Farrow, D. O. Scanlon, P. P. Wells, M. Bowker, S. F. Parker and C. R. A. Catlow, *Surf. Sci.*, 2016, **653**, 45 LINK https://doi.org/10.1016/j.susc.2016.05.002

5. A. Chutia, I. P. Silverwood, M. R. Farrow, D. O. Scanlon, P. P. Wells, M. Bowker, S. F. Parker and C. R. A. Catlow, *Surf. Sci.*, 2016, **653**, LINK https://doi.org/10.1016/j.susc.2016.05.002

6. A. Chutia, D. J. Willock and C. R. A. Catlow, *Faraday Discuss.*, 2018, **208**, 123 LINK https://doi.org/10.1039/c8fd00002f

7. S. M. Rogers, C. R. A. Catlow, C. E. Chan-Thaw, A. Chutia, N. Jian, R. E. Palmer, M. Perdjon, A. Thetford, N. Dimitratos, A. Villa and P. P. Wells, *ACS Catal.*, 2017, **7**, (4), 2266 LINK https://doi.org/10.1021/acscatal.6b03190

8. A. Chutia, I. Hamada and M. Tokuyama, *Surf. Sci.*, 2014, **628**, 116 LINK https://doi.org/10.1016/j.susc.2014.05.012

9. E. K. Dann, E. K. Gibson, R. H. Blackmore, C. R. A. Catlow, P. Collier, A. Chutia, T.

E. Erden, C. Hardacre, A. Kroner, M. Nachtegaal, A. Raj, S. M. Rogers, S. F. R. Taylor, P. Thompson, G. F. Tierney, C. D. Zeinalipour-Yazdi, A. Goguet and P. P. Wells, *Nat. Catal.*, 2019, **2**, (2), 157 LINK https://doi.org/10.1038/s41929-018-0213-3

10. A. Lahiri, A. Chutia, T. Carstens and F. Endres, *J. Electrochem. Soc.*, 2020, **167**, (11), 112501 LINK https://doi.org/10.1149/1945-7111/ab9e3c
11. N. C. Hernández, R. Grau-Crespo, N. H. de Leeuw and J. F. Sanz, *Phys. Chem. Chem. Phys.*, 2009, **11**, (26), 5246 LINK https://doi.org/10.1039/b820373c
12. R. Grau-crespo, H. De Leeuw, J. Fdez and N. C. Herna 2009, 5246 LINK https://doi.org/10.1039/b820373c
13. R. Grau-Crespo, N. Cruz Hernandez, J. F. Sanz and N. H. de Leeuw, *J. Phys. Chem. C*, 2007, **111**, (111), 10448
14. S. S. Tafreshi, A. Roldan, N. Y. Dzade and N. H. De Leeuw, *Surf. Sci.*, 2014, **622**, 1 LINK https://doi.org/10.1016/j.susc.2013.11.013
15. P. J. Bryant, P. L. Gutshall and L. H. Taylor, *Wear*, 1964, **7**, (1), 118 LINK https://doi.org/10.1016/0043-1648(64)90083-3
16. A. W. Hull, *Phys. Rev. B*, 1917, **10**, (6), 661 LINK https://doi.org/10.1017/S0885715600016018
17. J. D. Bernal, *Proc. R. Soc. A Math. Phys. Eng. Sci.*, 1924, **106**, 749
18. O. Hassel and H. Mark, *Zeitschrift für Phys.*, 1924, **25**, 317 LINK https://doi.org/10.1007/BF01327534
19. D. L. A. Taylor, *Nature*, 1940, **146**, 130
20. H. Lipson and A. R. Stokes, *Proc. R. Soc. London. Ser. A. Math. Phys. Sci.*, 1942,

181, (984), 101 LINK https://doi.org/10.1098/rspa.1942.0063

21. G. E. Bacon, *Acta Crystallogr.*, 1952, **5**, (4), 492 LINK https://doi.org/10.1107/s0365110x52001416

22. H. Jagodzinski, *Acta Crystallogr.*, 1949, **2**, (5), 298 LINK https://doi.org/10.1107/s0365110x49000771

23. H. -P Boehm and U. Hofmann, *Zeitschrift für Anorg. und Allg. Chemie*, 1955, **278**, (1–2), 58 LINK https://doi.org/10.1002/zaac.19552780109

24. F. Laves and Y. Baskin, *Zeitschrift fur Krist. - New Cryst. Struct.*, 1956, **107**, (5–6), 337 LINK https://doi.org/10.1524/zkri.1956.107.5-6.337

25. J. C. Charlier, X. Gonze and J. P. Michenaud, *Carbon N. Y.*, 1994, **32**, (2), 289 LINK https://doi.org/10.1016/0008-6223(94)90192-9

26. G. E. Washburn, *Ann. Phys.*, 1914, **48**, 236

27. V. E. Ryschkewitsch, *Zeitschrift fur Electrochem. und Angew. Phys. chemie*, 1922, **29**, 474

28. K. S. Krishnan and N. Ganguli, *Nature*, 1939, **144**, 667

29. E. Kogan and V. M. Silkin, *Phys. Status Solidi Basic Res.*, 2017, **254**, (9), 1700035 LINK https://doi.org/10.1002/pssb.201700035

30. C. A. Coulson, *NatureGroup*, 1947, **159**, 265

31. P. R. Wallace, *Phys. Rev.*, 1947, **71**, (9), 622 LINK https://doi.org/10.2208/jsceja.64.452

32. I. C. Brownlie, J. R. Fryer and G. Webb, *J. Catal.*, 1969, **14**, (3), 263 LINK https://doi.org/10.1016/0021-9517(69)90435-7

33. G. R. Hennig, *J. Inorg. Nucl. Chem.*, 1962, **24**, (9), 1129 LINK

https://doi.org/10.1016/0022-1902(62)80258-9

34. W. Li, C. Han, W. Liu, M. Zhang and K. Tao, *Catal. Today*, 2007, **125**, (3–4), 278 LINK https://doi.org/10.1016/j.cattod.2007.01.035

35. M. Chen, B. Lou, Z. Ni and B. Xu, *Electrochim. Acta*, 2015, **165**, 105 LINK https://doi.org/10.1016/j.electacta.2015.03.007

36. Y. Wen, K. He, Y. Zhu, F. Han, Y. Xu, I. Matsuda, Y. Ishii, J. Cumings and C. Wang, *Nat. Commun.*, 2014, **5**, (May), 1 LINK https://doi.org/10.1038/ncomms5033

37. A. Bhattacharya, A. Hazra, S. Chatterjee, P. Sen, S. Laha and I. Basumallick, *J. Power Sources*, 2004, **136**, 208 LINK https://doi.org/10.1016/j.jpowsour.2004.03.003

38. G. Zhang, C. Huang, R. Qin, Z. Shao, D. An, W. Zhang and Y. Wang, *J. Mater. Chem. A*, 2015, **3**, (9), 5204 LINK https://doi.org/10.1039/c4ta06076h

39. C. Srinivasan, *Curr. Sci.*, 2007, **92**, (10), 1338

40. K. S. Novoselov, D. Jiang, F. Schedin, T. J. Booth, V. V. Khotkevich, S. V. Morozov and A. K. Geim, *Proc. Natl. Acad. Sci. U. S. A.*, 2005, **102**, (30), 10451 LINK https://doi.org/10.1073/pnas.0502848102

41. A. Marinkas, F. Arena, J. Mitzel, G. M. Prinz, A. Heinzel, V. Peinecke and H. Natter, *Carbon N. Y.*, 2013, **58**, 139 LINK https://doi.org/10.1016/j.carbon.2013.02.043

42. N. M. Julkapli and S. Bagheri, *Int. J. Hydrogen Energy*, 2015, **40**, (2), 948 LINK https://doi.org/10.1016/j.ijhydene.2014.10.129

43. D. Pantea, H. Darmstadt, S. Kaliaguine, L. Sümmchen and C. Roy, *Carbon N. Y.*, 2001, **39**, (8), 1147 LINK https://doi.org/10.1016/S0008-6223(00)00239-6

44. L. J. Kennedy, J. J. Vijaya and G. Sekaran, *Mater. Chem. Phys.*, 2005, **91**, (2–3),

471 LINK https://doi.org/10.1016/j.matchemphys.2004.12.013

45. S. F. Parker, H. C. Walker, S. K. Callear, E. Grünewald, T. Petzold, D. Wolf, K. Möbus, J. Adam, S. D. Wieland, M. Jiménez-Ruiz and P. W. Albers, *Chem. Sci.*, 2019, **10**, (2), 480 LINK https://doi.org/10.1039/c8sc03766c

46. S. F. Parker, S. Imberti, S. K. Callear and P. W. Albers, *Chem. Phys.*, 2013, **427**, 44 LINK https://doi.org/10.1016/j.chemphys.2013.05.002

47. P. W. Albers, W. Weber, K. Kunzmann, M. Lopez and S. F. Parker, *Surf. Sci.*, 2008, **602**, (23), 3611 LINK https://doi.org/10.1016/j.susc.2008.10.006

48. P. W. Albers, J. Pietsch, J. Krauter and S. F. Parker, *Phys. Chem. Chem. Phys.*, 2003, **5**, (9), 1941 LINK https://doi.org/10.1039/b212210n

49. P. Albers, E. Auer, K. Ruth and S. F. Parker, *J. Catal.*, 2000, **196**, (1), 174 LINK https://doi.org/10.1006/jcat.2000.3021

50. S. F. Parker, K. P. J. Williams, P. Meehan, M. A. Adams and J. Tomkinson, *Appl. Spectrosc.*, 1994, **48**, (6), 669 LINK https://doi.org/10.1366/000370294774369027

51. I. K. M. Yu, X. Xiong, D. C. W. Tsang, Y. H. Ng, J. H. Clark, J. Fan, S. Zhang, C. Hu and Y. S. Ok, *Green Chem.*, 2019, **21**, (16), 4341 LINK https://doi.org/10.1039/c9gc00734b

52. S. Kundu, T. C. Nagaiah, X. Chen, W. Xia, M. Bron, W. Schuhmann and M. Muhler, *Carbon N. Y.*, 2012, **50**, (12), 4534 LINK https://doi.org/10.1016/j.carbon.2012.05.037

53. J. B. Donnet, *Carbon N. Y.*, 1982, **20**, (4), 267 LINK https://doi.org/10.1016/0008-6223(82)90002-1

54. R. D. Heidenreich, W. M. Hess and L. L. Ban, *J. Appl. Crystallogr.*, 1968, **1**, (1), 1 LINK https://doi.org/10.1107/s0021889868004930

55. C. Jäger, T. Henning, R. Schlögl and O. Spillecke, *J. Non. Cryst. Solids*, 1999, **258**, 161 LINK https://doi.org/10.1016/S0022-3093(99)00436-6

56. H. V. Drushel and J. V. Hallum, *J. Phys. Chem.*, 1959, **62**, (12), 1502 LINK https://doi.org/10.1021/j150570a008

57. M. L.DevineyJr., *Adv. Colloid Interface Sci.*, 1969, **2**, (3), 238

58. V. A. Garten and D. E. Weiss, *Aust. J. Chem.*, 1957, **10**, (3), 309

59. M. L. Studebaker, E. W. D. Huffman, A. C. Wolfe and L. G. Nabors, *Ind. Eng. Chem.*, 1956, **48**, (1), 162 LINK https://doi.org/10.1021/ie50553a044

60. H.-P. Boehm, E. Diehl, W. Heck and R. Sappok, *Angew. Chemie Int. Ed. English*, 1964, **3**, (10), 669 LINK https://doi.org/10.1002/anie.196406691

61. H. P. Boehm, *Carbon N. Y.*, 1994, **32**, (5), 759 LINK https://doi.org/10.1016/0008-6223(94)90031-0

62. B. R. Puri, *Carbon N. Y.*, 1966, **4**, (3), 391 LINK https://doi.org/10.1016/0008-6223(66)90052-2

63. J. Li, F. He, Y. Luo, Y. Yin, X. Dai and X. Liao, *Plasma Sci. Technol.*, 2003, **5**, (3), 1815 LINK https://doi.org/10.1088/1009-0630/5/3/010

64. D. Pantea, H. Darmstadt, S. Kaliaguine and C. Roy, *Appl. Surf. Sci.*, 2003, **217**, (1–4), 181 LINK https://doi.org/10.1016/S0169-4332(03)00550-6

65. B. C. Brodie, *R. Soc. London*, 1858, **149**, 249 LINK http://rstl.royalsocietypublishing.org/content/149/249.full.pdf+html

66. S. Gilje, S. Han, M. Wang, K. L. Wang and R. B. Kaner, *Nano Lett.*, 2007, **7**, (11),

3394 LINK https://doi.org/10.1021/nl0717715

67. T. Nakajima, A. Mabuchi and R. Hagiwara, *Carbon N. Y.*, 1988, **26**, (3), 357 LINK https://doi.org/10.1016/0008-6223(88)90227-8

68. R. Hummers, W. S.; Offeman and E., *J. Am. Chem. Soc.*, 1957, **80**, 1339 LINK https://pubs.acs.org/sharingguidelines

69. T. Nakajima and Y. Matsuo, *Carbon N. Y.*, 1994, **32**, (3), 469 LINK https://doi.org/10.1016/0008-6223(94)90168-6

70. C. Hontoria-Lucas, A. J. Lopez-Peinado and J. D. D. Lopez-Gonzalez, *Carbon N. Y.*, 1995, **33**, (11), 1585 LINK https://doi.org/10.1248/jhs1956.22.20

71. A. Lerf, H. He, M. Forster and J. Klinowski, *J. Phys. Chem. B*, 1998, **102**, (23), 4477 LINK https://doi.org/10.1021/jp9731821

72. Y. Han and Y. Lu, *Carbon N. Y.*, 2007, **45**, (12), 2394 LINK https://doi.org/10.1016/j.carbon.2007.07.007

73. V. S. Talanov, G. G. Talanova and K. B. Yatsimirskii, *Theor. Exp. Chem.*, 1996, **32**, (4), 221

74. D. W. Lee, L. De Los Santos V., J. W. Seo, L. L. Felix, A. Bustamante D., J. M. Cole and C. H. W. Barnes, *J. Phys. Chem. B*, 2010, **114**, (17), 5723 LINK https://doi.org/10.1021/jp1002275

75. W. Gao, L. B. Alemany, L. Ci and P. M. Ajayan, *Nat. Chem.*, 2009, **1**, (5), 403 LINK https://doi.org/10.1038/nchem.281

76. I. Efremenko and M. Sheintuch, *Langmuir*, 2006, **22**, (8), 3614 LINK https://doi.org/10.1021/la052100u

77. T. J. Bandosz, J. Jagiello and J. A. Schwarz, *Anal. Chem.*, 1992, **64**, (8), 891 LINK

https://doi.org/10.1021/ac00032a012

78. J. S. Noh and J. A. Schwarz, *Carbon N. Y.*, 1990, **28**, (5), 675 LINK https://doi.org/10.1016/0008-6223(90)90069-B

79. J. L. Figueiredo, M. F. R. Pereira, M. M. A. Freitas and J. J. M. Órfão, *Carbon N. Y.*, 1999, **37**, (9), 1379 LINK https://doi.org/10.1016/S0008-6223(98)00333-9

80. D. D. Edie, *Carbon N. Y.*, 1998, **36**, (4), 345 LINK https://doi.org/https://doi.org/10.1016/S0008-6223(97)00185-1

81. K. Acatay, 'Carbon Fibers', ed. M. M. M. Özgür Seydibeyoğlu, Amar K. Mohanty,'Fiber Technol. Fiber-Reinforced Compos.', Elsevier Ltd, 2017 LINK https://doi.org/10.1016/B978-0-08-101871-2.00006-0

82. M. S. Dresselhaus, G. Dresselhaus, K. Sugihara, I. L. Spain and H. A. Goldberg, 'Synthesis of Graphite Fibers and Filaments', in 'Graph. Fibers Filaments', Springer Series in Materials Science, 1988 LINK https://doi.org/10.1007/978-3-642-83379-3_2

83. R. H. Bradley, X. Ling and I. Sutherland, *Carbon N. Y.*, 1993, **31**, (7), 1115 LINK https://doi.org/10.1016/0008-6223(93)90064-H

84. J. Gulyás, E. Földes, A. Lázár and B. Pukánszky, *Compos. Part A Appl. Sci. Manuf.*, 2001, **32**, (3–4), 353 LINK https://doi.org/10.1016/S1359-835X(00)00123-8

85. L. Szabó, R. Milotskyi, T. Tsukegi, N. Wada and K. Takahashi, *Appl. Surf. Sci.*, 2019, **494**, (June), 315 LINK https://doi.org/10.1016/j.apsusc.2019.07.185

86. A. I. Medalia, D. Rivin and D. R. Sanders, *Sci. Total Environ.*, 1983, **31**, (1), 1 LINK https://doi.org/10.1016/0048-9697(83)90053-0

87. B. R. Stanmore, J. F. Brilhac and P. Gilot, *Carbon N. Y.*, 2001, **39**, (15), 2247 LINK

https://doi.org/10.1016/S0008-6223(01)00109-9

88. D. S. Su, R. E. Jentoft, J. O. Müller, D. Rothe, E. Jacob, C. D. Simpson, Ž. Tomović, K. Müllen, A. Messerer, U. Pöschl, R. Niessner and R. Schlögl, *Catal. Today*, 2004, **90**, (1–2), 127 LINK https://doi.org/10.1016/j.cattod.2004.04.017

89. S. Hamad, J. A. Mejias, S. Lago, S. Picaud and P. N. M. Hoang, *J. Phys. Chem. B*, 2004, **108**, (17), 5405 LINK https://doi.org/10.1021/jp037589j

90. W. K. P. Hohenberg, *Phys. Rev. B*, 1964, **136**, B 864 LINK https://doi.org/10.1103/PhysRevB.7.1912

91. W. Kohn and L. J. Sham, *Phys. Rev.*, 1965, **140**, (4A),

92. A. D. Becke, *J. Chem. Phys.*, 2014, **140**, LINK https://doi.org/10.1063/1.4869598

93. R. G. Parr and W. Yang, 'Density-Functional Theory of Atoms and Molecules', 'Oxford Univ. Press', Oxford University Press, 1989

94. I. N. Levine, 'Quantum Chemistry', 5th Ed., Prentice Hall, Upper Saddle River, New Jersey, 2000

95. S. Kurth and J. Perdew, *Int. J. Quantum Chem.*, 2000, **77**, 814 LINK https://doi.org/10.1002/(SICI)1097-461X(2000)77:5<814::AID-QUA3>3.0.CO;2-F

96. S. H. Vosko, L. Wilk and M. Nusair, *Can. J. Phys.*, 1980, **58**, (8), 1200 LINK https://doi.org/10.1139/p80-159

97. J. P. Perdew and A. Zunger, *Phys. Rev. B*, 1981, **23**, (10), 5048 LINK https://doi.org/10.1103/PhysRevB.23.5048

98. J. P. Perdew and Y. Wang, *Phys. Rev. B*, 1992, **45**, (23), 13244 LINK https://doi.org/10.1103/PhysRevB.45.13244

99. J. P. Perdew, K. Burke and M. Ernzerhof, *Phys. Rev. Lett.*, 1996, **77**, (18), 3865 LINK https://doi.org/10.1103/PhysRevLett.77.3865

100. B. Hammer, L. Hansen and J. Nørskov, *Phys. Rev. B*, 1999, **59**, (11), 7413 LINK https://doi.org/10.1103/PhysRevB.59.7413

101. Y. Zhang and W. Yang, *Phys. Rev. Lett.*, 1998, **80**, (4), 890 LINK https://doi.org/10.1103/PhysRevLett.80.890

102. G. I. Csonka, J. P. Perdew, A. Ruzsinszky, P. H. T. Philipsen, S. Lebègue, J. Paier, O. A. Vydrov and J. G. Ángyán, *Phys. Rev. B - Condens. Matter Mater. Phys.*, 2009, **79**, (15), 155107 LINK https://doi.org/10.1103/PhysRevB.79.155107

103. M. Dion, H. Rydberg, E. Schröder, D. C. Langreth and B. I. Lundqvist, *Phys. Rev. Lett.*, 2004, **92**, (24), 1 LINK https://doi.org/10.1103/PhysRevLett.92.246401

104. K. Lee, É. D. Murray, L. Kong, B. I. Lundqvist and D. C. Langreth, *Phys. Rev. B - Condens. Matter Mater. Phys.*, 2010, **82**, (8), 081101 LINK https://doi.org/10.1103/PhysRevB.82.081101

105. T. Thonhauser, V. R. Cooper, S. Li, A. Puzder, P. Hyldgaard and D. C. Langreth, *Phys. Rev. B - Condens. Matter Mater. Phys.*, 2007, **76**, (12), 1 LINK https://doi.org/10.1103/PhysRevB.76.125112

106. I. Hamada, *Phys. Rev. B - Condens. Matter Mater. Phys.*, 2014, **89**, (12), 121103 LINK https://doi.org/10.1103/PhysRevB.89.121103

107. Y. Zhao and D. G. Truhlar, *J. Chem. Phys.*, 2006, **125**, (19), 194101 LINK https://doi.org/10.1063/1.2370993

108. Y. Zhao and D. G. Truhlar, *Theor. Chem. Acc.*, 2008, **120**, (1–3), 215 LINK https://doi.org/10.1007/s00214-007-0310-x

109. J. Tao and J. P. Perdew 2003, (October), 3 LINK https://doi.org/10.1103/PhysRevLett.91.146401

110. J. P. Perdew, A. Ruzsinszky, G. I. Csonka, L. A. Constantin and J. Sun, *Phys. Rev. Lett.*, 2009, **103**, (2), 026403 LINK https://doi.org/10.1103/PhysRevLett.103.026403

111. A. Becke, *J. Chem. Phys.*, 1993, **98**, 5648

112. A. J. Cohen and N. C. Handy, *Mol. Phys.*, 2001, **99**, (7), 607 LINK https://doi.org/10.1080/00268970010023435

113. J. Heyd, G. E. Scuseria and M. Ernzerhof, *J. Chem. Phys.*, 2003, **118**, (18), 8207 LINK https://doi.org/10.1063/1.1564060

114. A. V. Krukau, O. A. Vydrov, A. F. Izmaylov and G. E. Scuseria, *J. Chem. Phys.*, 2006, **125**, (22), 224106 LINK https://doi.org/10.1063/1.2404663

115. C. Adamo and V. Barone, *J. Chem. Phys.*, 1999, **110**, (13), 6158 LINK https://doi.org/10.1063/1.478522

116. T. Yanai, D. P. Tew and N. C. Handy, *Chem. Phys. Lett.*, 2004, **393**, (1–3), 51 LINK https://doi.org/10.1016/j.cplett.2004.06.011

117. T. M. Henderson, A. F. Izmaylov, G. Scalmani and G. E. Scuseria, *J. Chem. Phys.*, 2009, **131**, (4), 044108 LINK https://doi.org/10.1063/1.3185673

118. D. Appy, H. Lei, C. Z. Wang, M. C. Tringides, D. J. Liu, J. W. Evans and P. A. Thiel, *Prog. Surf. Sci.*, 2014, **89**, (3–4), 219 LINK https://doi.org/10.1016/j.progsurf.2014.08.001

119. D. M. Duffy and J. A. Blackman, *Phys. Rev. B*, 1998, **58**, (11), 7443 LINK https://doi.org/10.1016/S0039-6028(98)00543-3

120. B. Delley, *J. Chem. Phys.*, 1990, **92**, (1), 508 LINK https://doi.org/10.1063/1.458452

121. B. Delley, *J. Chem. Phys.*, 2000, **113**, (18), 7756 LINK https://doi.org/10.1063/1.1316015

122. H. Valencia, A. Gil and G. Frapper, *J. Phys. Chem. C*, 2010, **114**, (33), 14141 LINK https://doi.org/10.1021/jp103445v

123. R. Hoffmann and W. N. Lipscomb, *J. Chem. Phys.*, 1962, **36**, (8), 2179 LINK https://doi.org/10.1063/1.1732849

124. R. Hoffmann and W. N. Lipscomb, *J. Chem. Phys.*, 1962, **36**, (12), 3489 LINK https://doi.org/10.1063/1.1732484

125. R. Hoffmann, *J. Chem. Phys.*, 1963, **39**, (6), 1397 LINK https://doi.org/10.1063/1.1734456

126. C. Mealli and D. M. Proserpio, *J. Chem. Educ.*, 1990, **67**, (5), 399 LINK https://doi.org/10.1021/ed067p399

127. K. Nakada and A. Ishii, *Solid State Commun.*, 2011, **151**, (1), 13 LINK https://doi.org/10.1016/j.ssc.2010.10.036

128. M. Manadé, F. Viñes and F. Illas, *Carbon N. Y.*, 2015, **95**, 525 LINK https://doi.org/10.1016/j.carbon.2015.08.072

129. D. M. Duffy and J. A. Blackman, *Surf. Sci.*, 1998, **415**, (3), LINK https://doi.org/10.1016/S0039-6028(98)00543-3

130. P. Jensen, X. Blase and P. Ordejón, *Surf. Sci.*, 2004, **564**, (1–3), 173 LINK https://doi.org/10.1016/j.susc.2004.06.188

131. G. M. Wang, J. J. BelBruno, S. D. Kenny and R. Smith, *Surf. Sci.*, 2003, **541**, (1–

3), 91 LINK https://doi.org/10.1016/S0039-6028(03)00837-9

132. T. P. Hardcastle, C. R. Seabourne, R. Zan, R. M. D. Brydson, U. Bangert, Q. M. Ramasse, K. S. Novoselov and A. J. Scott, *Phys. Rev. B - Condens. Matter Mater. Phys.*, 2013, **87**, (19), 1 LINK https://doi.org/10.1103/PhysRevB.87.195430
133. A. Tkatchenko and M. Scheffler, *Phys. Rev. Lett.*, 2009, **102**, (7), 073005 LINK https://doi.org/10.1103/PhysRevLett.102.073005
134. S. J. Clark, M. D. Segall, C. J. Pickard, P. J. Hasnip, M. J. Probert, K. Refson and M. C. Payne, *Zeitschrift für Krist.*, 2005, **220**, (5-6–2005), 567 LINK https://doi.org/10.1524/zkri.220.5.567.65075
135. J. Engel, S. Francis and A. Roldan, *Phys. Chem. Chem. Phys.*, 2019, **21**, (35), 19011 LINK https://doi.org/10.1039/c9cp03066b
136. G. F. Wei and Z. P. Liu, *Chem. Sci.*, 2015, **6**, (2), 1485 LINK https://doi.org/10.1039/c4sc02806f
137. Z. Bo, X. Guo, X. Wei, H. Yang, J. Yan and K. Cen, *Phys. E Low-Dimensional Syst. Nanostructures*, 2019, **109**, (2), 156 LINK https://doi.org/10.1016/j.physe.2019.01.012
138. A. Caglar, D. Düzenli, I. Onal, I. Tezsevin, O. Sahin and H. Kivrak, *Int. J. Hydrogen Energy*, 2020, **45**, (1), 490 LINK https://doi.org/10.1016/j.ijhydene.2019.10.163
139. F. Montejo-Alvaro, J. Oliva, A. Zarate, M. Herrera-Trejo, H. M. Hdz-García and A. I. Mtz-Enriquez, *Phys. E Low-Dimensional Syst. Nanostructures*, 2019, **110**, (October 2018), 52 LINK https://doi.org/10.1016/j.physe.2019.02.005
140. F. Banhart, J. Kotakoski and A. V. Krasheninnikov, *ACS Nano*, 2011, **5**, (1), 26

LINK https://doi.org/10.1021/nn102598m

141. R. Zan, Q. M. Ramasse, U. Bangert and K. S. Novoselov, *Nano Lett.*, 2012, **12**, (8), 3936 LINK https://doi.org/10.1021/nl300985q

142. A. V. Krasheninnikov, P. O. Lehtinen, A. S. Foster, P. Pyykkö and R. M. Nieminen, *Phys. Rev. Lett.*, 2009, **102**, (12), 126807 LINK https://doi.org/10.1103/PhysRevLett.102.126807

143. A. V. Krasheninnikov and R. M. Nieminen, *Theor. Chem. Acc.*, 2011, **129**, (3–5), 625 LINK https://doi.org/10.1007/s00214-011-0910-3

144. D. Sen, R. Thapa and K. K. Chattopadhyay, *Int. J. Hydrogen Energy*, 2013, **38**, (7), 3041 LINK https://doi.org/10.1016/j.ijhydene.2012.12.113

145. Y. Hamamoto, S. A. Wella, K. Inagaki, F. Abild-Pedersen, T. Bligaard, I. Hamada and Y. Morikawa, *Phys. Rev. B*, 2020, **102**, (7), 75408 LINK https://doi.org/10.1103/PhysRevB.102.075408

146. H. Wang, T. Maiyalagan and X. Wang, *ACS Catal.*, 2012, **2**, (5), 781 LINK https://doi.org/10.1021/cs200652y

147. Z. Zuo, Z. Jiang and A. Manthiram, *J. Mater. Chem. A*, 2013, **1**, (43), 13476 LINK https://doi.org/10.1039/c3ta13049e

148. H. Pinto and A. Markevich, *Beilstein J. Nanotechnol.*, 2014, **5**, (1), 1842 LINK https://doi.org/10.3762/bjnano.5.195

149. X. Ren, J. Zhu, F. Du, J. Liu and W. Zhang, *J. Phys. Chem. C*, 2014, **118**, (39), 22412 LINK https://doi.org/10.1021/jp505876z

150. B. R. Sathe, X. Zou and T. Asefa, *Catal. Sci. Technol.*, 2014, **4**, (7), 2023 LINK https://doi.org/10.1039/c4cy00075g

151. L. K. Putri, W. J. Ong, W. S. Chang and S. P. Chai, *Appl. Surf. Sci.*, 2015, **358**, 2 LINK https://doi.org/10.1016/j.apsusc.2015.08.177

152. C. Xu, Y. Su, D. Liu and X. He, *Phys. Chem. Chem. Phys.*, 2015, **17**, (38), 25440 LINK https://doi.org/10.1039/c5cp04211a

153. X. F. Li, K. Y. Lian, L. Liu, Y. Wu, Q. Qiu, J. Jiang, M. Deng and Y. Luo, *Sci. Rep.*, 2016, **6**, (October 2015), 1 LINK https://doi.org/10.1038/srep23495

154. S. Park, Y. Hu, J. O. Hwang, E. S. Lee, L. B. Casabianca, W. Cai, J. R. Potts, H. W. Ha, S. Chen, J. Oh, S. O. Kim, Y. H. Kim, Y. Ishii and R. S. Ruoff, *Nat. Commun.*, 2012, **3**, 1 LINK https://doi.org/10.1038/ncomms1643

155. S. Agnoli and M. Favaro, *J. Mater. Chem. A*, 2016, **4**, (14), 5002 LINK https://doi.org/10.1039/c5ta10599d

156. L. Zhang and Z. Xia, *J. Phys. Chem. C*, 2011, **115**, (22), 11170 LINK https://doi.org/10.1021/jp201991j

157. S. Ullah, P. A. Denis and F. Sato, *ChemPhysChem*, 2017, **18**, (14), 1864 LINK https://doi.org/10.1002/cphc.201700278

158. Q. Zhou, L. Yuan, X. Yang, Z. Fu, Y. Tang, C. Wang and H. Zhang, *Chem. Phys.*, 2014, **440**, 80 LINK https://doi.org/10.1016/j.chemphys.2014.06.016

159. G. Wu, D. Li, C. Dai, D. Wang and N. Li, *Langmuir*, 2008, **24**, (7), 3566 LINK https://doi.org/10.1021/la7029278

160. M. N. Groves, A. S. W. Chan, C. Malardier-Jugroot and M. Jugroot, *Chem. Phys. Lett.*, 2009, **481**, (4–6), 214 LINK https://doi.org/10.1016/j.cplett.2009.09.074

161. T. Kropp and M. Mavrikakis, *ACS Catal.*, 2019, **9**, (8), 6864 LINK https://doi.org/10.1021/acscatal.9b01944

162. J. Ni, M. Quintana and S. Song, *Phys. E Low-Dimensional Syst. Nanostructures*, 2020, **116**, (July 2019), 113768 LINK https://doi.org/10.1016/j.physe.2019.113768

163. A. Chutia, Z. Zhu, R. Sahnoun, H. Tsuboi, M. Koyama, N. Hatekeyama, A. Endou, H. Takaba, M. Kubo, C. A. Del Carpio and A. Miyamoto, *Jpn. J. Appl. Phys.*, 2008, **47**, (4), 3147 LINK https://doi.org/10.1143/jjap.47.3147

164. A. Chutia, R. Sahnoun, R. C. Deka, Z. G. Zhu, H. Tsuboi, H. Takaba and A. Miyamoto, *Phys. B-Condensed Matter*, 2011, **406**, (9), 1665 LINK https://doi.org/10.1016/j.physb.2010.01.012

165. A. Chutia, F. Cimpoesu, H. Tsuboi and A. Miyamoto, *Chem. Phys. Lett.*, 2011, **503**, (1–3), 91 LINK https://doi.org/DOI 10.1016/j.cplett.2010.12.057

166. Y. Chen, W. Zhang, S. Yang, A. Hobiny, A. Alsaedi and X. Wang, *Sci. China Chem.*, 2016, **59**, (4), 412 LINK https://doi.org/10.1007/s11426-015-5549-9

167. S. Kim, K. C. Kim, S. W. Lee and S. S. Jang, *Phys. Chem. Chem. Phys.*, 2016, **18**, (30), 20600 LINK https://doi.org/10.1039/c6cp02692c

168. N. Jin, J. Han, H. Wang, X. Zhu and Q. Ge, *Int. J. Hydrogen Energy*, 2015, **40**, (15), 5126 LINK https://doi.org/10.1016/j.ijhydene.2015.02.101

169. C. Cui, M. Sun, X. Zhu, J. Han, H. Wang and Q. Ge, *Catalysts*, 2020, **10**, (2), 156 LINK https://doi.org/10.3390/catal10020156

170. L. Sahoo, S. Mondal, A. Gloskovskii, A. Chutia and U. K. Gautam, *J. Mater. Chem. A*, 2021, **9**, 10966 LINK https://doi.org/10.1039/d0ta12618g

171. L. Rout, A. Kumar, R. S. Dhaka, G. N. Reddy, S. Giri and P. Dash, *Appl. Catal. A Gen.*, 2017, **538**, 107 LINK https://doi.org/10.1016/j.apcata.2017.03.017

172. M. A. Caro, A. Aarva, V. L. Deringer, G. Csányi and T. Laurila, *Chem. Mater.*, 2018, **30**, (21), 7446 LINK https://doi.org/10.1021/acs.chemmater.8b03353

173. R. Ranganathan, S. Rokkam, T. Desai and P. Keblinski, *Carbon N. Y.*, 2017, **113**, 87 LINK https://doi.org/10.1016/j.carbon.2016.11.024

The Author

Arunabhiram Chutia received his PhD in theoretical and computational chemistry from the Graduate School of Engineering, Tohoku University, Japan. Thereafter, he undertook his postdoctoral research in materials science and heterogenous/homogenous catalysis at WPI-Advanced Institute of Materials Research, Institute of Fluid Science (Tohoku University), at the Fuel Cell Nanomaterials Centre (Yamanashi University) and jointly at University College London and the UK catalysis Hub in the UK. Currently, he is a senior lecturer in chemistry and leads the molecular surface chemistry group (www.molsurfchem.org) at the University of Lincoln.